2011 International Symposium on Nonlinear Theory and its Applications
NOLTA2011, Kobe, Japan, September 4-7, 2011

Cortical microcircuits have no distinguished role in LSM information processing

Viktor Saase and Ruedi Stoop

Institute of Neuroinformatics, University of Zurich and ETH Zurich
Winterthurerstr. 190, 8057 Zrich
Email: saase@student.ethz.ch, ruedi@ini.phys.ethz.ch

Abstract—Cortical columns and their typical wiring are a puzzling phenomenon that is generally interpreted to have computational benefits. Echo State or Liquid State Machines are recurrent neural network paradigms that have been proven successful in the learning of action sequences, an aspect crucial to robotics. We scrutinize the recent assertion made by Mass and scholars that when to these frameworks biologically inspired neural network topologies are overlaid, they will increase their efficiency. A vast parameter survey performed on typical applications does, however, not support this hypothesis.

1. Echo state and liquid state concepts

Cortical columns and their typical wiring are a puzzling phenomenon which is generally interpreted as to having some beneficial computational effect. It has already been remarked that Echo State Machines (ESN) with analog neurons and sigmoidal transfer functions show little performance sensitivity with respect to changes of the reservoir topology [1, 2]. In the quest of understanding the brain, following the idea to take the recurrently connected cortex as the blueprint for artificial neural networks, spiking neurons were introduced into the reservoir. This led to the "Liquid State Machines" (LSM) network paradigm ([3]). In these networks, a marked performance increase was reported if within their reservoir a refining topology was implemented that in some sense was 'close' to that found in the mammalian cortex [3, 4, 5, 6]. This interesting phenomenon was investigated in details in [6], by comparing an LSM endowed with a layering connectivity as dealt with in cortex, with LSM networks based on random wiring. For the layered network, a significantly improved computational performance was reported. Recent attempts [7, 8] to resolve the apparent contradiction between ESN and LSM performance attributed the phenomenon to the difference between the hyperbolic tangent vs. the Heaviside transfer function, i.e. to analog vs. digital/spiking neuronal information processing used in these paradigms. One finding was that LSM built on spiking neurons with digital membrane potential, were superior to fully analog neuron based LSM, particularly in conditions of sparse connectivity (typically 3 synapses/neuron) or sparse activity (typical for biological conditions), the reason being that the former more easily reach the region of optimal synaptic input. This argument, however, fails in the case of LSM built on spiking neurons with a continuous membrane potential.

In our contribution, we will follow and expand the approach taken by [6]. Contrary to the academic focus exhibited in their paper, here we critically re-evaluate their findings, claims and extrapolations in the application-centered context. As the general result, our experiments fail to confirm a straightforward extrapolation of their claims to the application context. The comparisons we perform had in some cases to remain qualitative, as we use different benchmark tasks and perform extended topological surveys. Both is necessary to prove that our observations are robust with respect to real world perceptional tasks and that they are salient in the context of machine learning. Since our focus is on neural architectures with a biological blueprint, we focus on spiking neural networks. Our overall finding across all benchmarks and a great variety of networks is that biologically motivated and random network topologies perform essentially equally well, which corroborates an original findings by [1].

A schematic overview on the ESN/LSM is given in Fig. 1. Reservoir neurons receive external input by the signal and recurrent input from other reservoir neurons. The

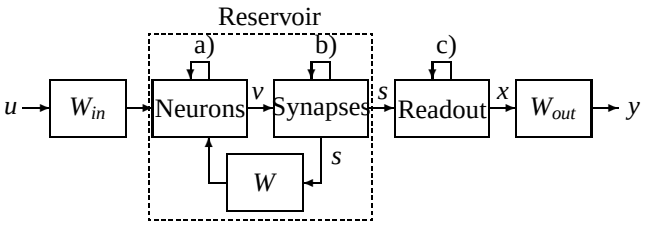

Figure 1: LSM model. Stimulus u fed into the reservoir should be associated with the 'correct' output y. The recurrent reservoir topology is encoded by matrix W. The matrix W_{out} is trained.

network topology we study is captured in the connection matrix W, the entries of which are the synaptic weights. For a network realization, only the connection *probabilities* will be prescribed, contrary to what the term 'cortical microcircuit' - the term abundantly used in [6] - might evoke otherwise. Excitatory (inhibitory) neurons, as the coarsest characterization of structure within the reservoir, are implemented by positive (negative, respectively) weights.

In the ESN/LSM context, learning is a supervised pro-

cess aiming at associating k pairs of input / output sequences $\{u(t)_i\,, y_d(t)_i\}_{i\in\{1,..,k\}}$ of individual sequence length T_i (so that $t \in \{1,..,T_i\}$). Upon stimulation by $u(t)_j$, the liquid reservoir of M neurons will generate a state vector $x(t)_j$. Let $T > \max_i(T_i)$ denote a maximal time of observation, and let X be the $k \times T$-matrix of liquid states, where T is the number of the reservoir neurons to be read out. Let similarly denote $Y_d = \{y_d(t)\}_j$ the $k \times T$ Matrix of the desired associated pattern indexed by j.

To approximate the desired relation $W^{out}x_i(t) \simeq y_{i_d}(t)$, by using the (Moore-Penrose) pseudo-inverse X^+ of X, the least-squares optimized read-out matrix

$$W^{out} \simeq Y_d X^+$$

is obtained.

As a practical example, we consider the learning of the response consisting in a temporal pattern $y_d(t)$ of length $T = 100$. During the training phase, the input and the desired output signal are fed into the reservoir. After a transient phase, the optimized output matrix W^{out} is obtained as the pseudo-inverse of the matrix of dimension $T\times M$ (where M is the dimension of the output vector, often equal to T), applied to the desired output vector $y_d(t)$ of dimension T. During recall, from the input signal via the reservoir read by the optimized readout neurons, the desired output should emerge. For the learning of a set of cardinality k of patterns, the reservoir is trained by using one of the patterns at random. After this period, the optimization involves taking the pseudo-inverse of the $T \times M$-dimensional matrix X^+, applied to the matrix of dimension $k \times T$ of the desired outputs Y_d. For associative tasks, a minimal distance classification is performed, usually by using the Euclidean distance.

In the networks investigated, two prominent models of neurons will be used alternatively.
The time evolution of the leaky integrate-and-fire neuron is defined by

$$v_i(t+\tau) = \exp(-\frac{\tau}{\tau_m})v_i(t) + \sum_j w_{ij}s_j(t) + \sum_k w_{in_{ik}}u_k(t).$$

Here, v_i is the membrane potential of the i'th neuron that decays exponentially in time with membrane time constant $\tau_m = 30$ ms. τ is the integration time-step. s_j is the postsynaptic potential at the synapses innervated by the j'th neuron, which is weighted by the synaptic efficiency w_{ij} mediating between the presynaptic neuron j and the postsynaptic neuron i. u_k denotes the k'th input component, weighted by $w_{in_{ik}}$, the weight of the k'th input component to neuron i. If v_i reaches the threshold $V_{thr} = 1$, a spike is triggered, which resets s_i to 1 and v_i to $V_{res} = 0$.
The time evolution of the fast-spiking simple Izhikevich neuron model [9] is given by the coupled equations

$$v_i(t+\tau) = v_i(t) + \tau\left[\frac{4}{100}\,v_i^2(t) + 5\,v_i(t) + 30\left(\sum_j w_{ij}s_j(t) + \sum_k w_{in_{ik}}u_k(t)\right) - r_i(t) + 152\right], \quad (1)$$

$$r_i(t+\tau) = r_i(t) + \tau\left[\frac{2}{100}v_i(t+\tau) - \frac{1}{10}\,r_i(t)\right]. \quad (2)$$

Here, r_i describes an additional continuous variable that controls the subthreshold dynamics and the refractoriness. After v_i has reached the threshold $V_{thr} = 30$, a spike is triggered, which resets s_i to 1, v_i to -65 and r_i to $r_i + 2$.

For both neuron types, the synapses are modeled by an exponential decaying postsynaptic potential of the form $s_i(t+\tau) = \exp\left(-\frac{\tau}{\tau_{Syn}}\right)s_i(t)$, with the synaptic decay time scale $\tau_{Syn} = 2$ ms. The axonal delays and the refractory periods are given by a fixed integration step of τ =2 ms, for all experiments.

We examine two reservoir topologies. In the first network model (EI), the biological blueprint is simplified to an excitatory and an inhibitory neuronal population and connections within and between them. In the second model (LEI), also a laminar organization of the neurons, as observed in the mammalian cortex, is implemented.

The biologically inspired network model used by [3] consists of a three-dimensional grid of neurons comprising $3 \times 3 \times 15 = 135$ neurons. The probability for a connection from neuron j to neuron i is given by $p_{con}(i,j) = C(i,j)\exp\left(-\frac{|\hat{x}_i-\hat{x}_j|^2}{\lambda^2}\right)$, where $|\hat{x}_i - \hat{x}_j|$ is the euclidean distance between the i'th and the j'th neurons' positions on a 3-dimensional grid representing the neural network. λ controls both the number and typical length of the connections. $C(i,j)$ establishes the desired bio-inspired excitatory-inhibitory connectivity, where the values $C(E,E) = 0.3$, $C(E,I) = 0.4$, $C(I,E) = 0.2$ and $C(I,I) = 0.1$ are used (where E indicates an excitatory, and I an inhibitory neuron). If a connection is made, the synaptic weights are chosen as $w(E,E) = 30$, $w(E,I) = -19$, $w(I,E) = 60$ and $w(I,I) = -19$. Rather than being geometrically segregated into layers, in this model the neurons are tagged with different properties. The model will be compared to a control network ('EI control') where C is uniformly set to 0.3 and where the synaptic weights are drawn from a uniform distribution on $[0,1]$, endowed with a sign to distinguish between inhibitory and excitatory neurons.

The more detailed cortex-inspired LEI network topology considered in the present context first by [6] consists of three layers (2/3, 4 and 5), each of them comprising an excitatory and an inhibitory population. As in the unlayered (EI) circuit, we chose a population consisting of 135 neurons. The connection probabilities and strengths between the populations were chosen as in [6]. The network is largely feed-forward. There are, however, recurrent connections within the individual layers. The topology also defines which neurons receive input and which neurons are to be read out from. Input to the network is mostly by means of projections to layer 4 (input stream 1 in [6]). Layer 2/3 plays the role of the hidden layer, while the output neurons are confined to layer 5. The translation from the dynamic synapses used in [6] to our exponential synapses is achieved by setting our synaptic weights equal to the steady

state strength U of [6]. The control network ('LEI control') is obtained by replacing at each synapse with a probability p the pre- and postsynaptic neurons by neurons chosen at random from the pooled neuronal ensembles of the same kind (excitatory or inhibitory). The rewiring procedure has the effect of merging the three layers, while retaining the overall connectivity and weight distribution between the excitatory and inhibitory populations. This allows us to examine the impact of the segregation of LSM into layers and interlayer connectivity for typical applications.

We used two ways of reading out the reservoir. Since the reservoir maintains the temporal information, in the original LSM design the readout is *memoryless*. For every input vector, an output vector is generated, allowing "anytime recognition" [3]. In classification tasks it is, however, necessary to have a memory span that is of the same order of size as the stimulus length. Otherwise, the LSM will confuse different stimuli classes when they contain similar parts (e.g. phonemes in speech recognition). As an alternative readout method, we used firing rates, computed over multiple input steps. For every stimulus, one output vector is generated consisting of the mean firing rates of the individual neurons, averaged over the whole stimulus length. Output is generated only after the stimulus has terminated. With this method, we observe greatly improved recognition, although it could not be considered a proper LSM procedure. We will refer to this readout as *integration* readout.

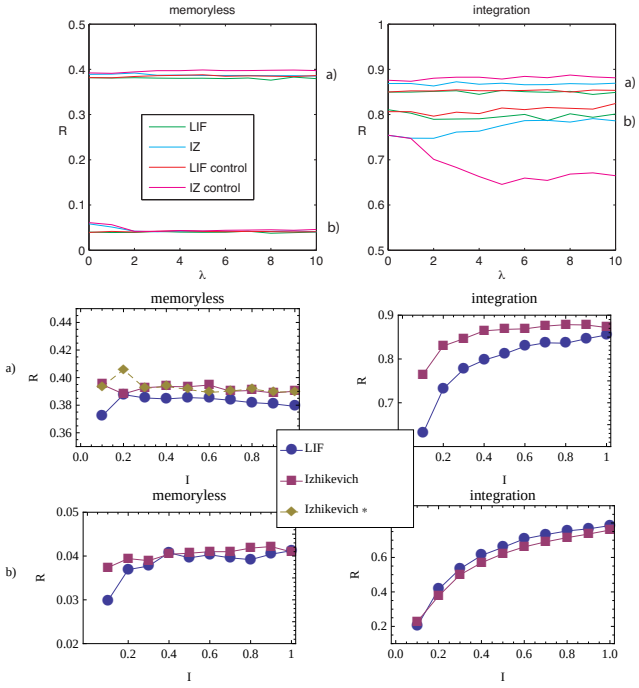

Figure 2: Recognition rate R of EI networks (a) Arabic Digit recognition, b) Auslan Sign recognition). Top panel: R as a function of connectivity λ (memoryless and integration readout). Lower panels: R as a function of input/reservoir size ratio I. Local connectivity ($\lambda = 2$) was used, except for Izhikevich * using no connections ($\lambda = 0$).

2. Results and Discussion

To assess the efficacy of the networks, and to attain a generality of observations, we use two common time series classification benchmarks. The single Arabic digit speech recognition task [10] comprises time series of 13 Mel Frequency Cepstral Coefficients (MFCC) for 10 classes of digits spoken by 88 subjects. The Australian Sign Language (Auslan) sign recognition task consist of time series of 22 parameters for 95 signs, recorded from digital glove and position tracker equipment from a native signer [11]. These tasks are directly related to the kind of computation that is expected from a spiking neural net, in contrast to abstract computations on spike trains which may include significant experimenter bias. The datasets are freely available [12]. The much larger number of classes in the Auslan task might be responsible for the generally weaker recognition rates the networks achieve in it. The remarkable consistency of our observations across both tasks yet is evidence for a strong independence of the observations from an optimization of network size to task size. Contrary to what is often claimed, local connections ($\lambda \approx 2$) render no advantage over other degrees of connectivity, see Fig.2, upper panel . Notably, not connecting the neurons at all does not lead to a decrease in the recognition rate of the LSM, suggesting that no integration or computation is owed to synaptic interaction. This has previously been observed by [13]. Connections can even lead to worse performance in the more realistic Izhikevich neuron model. The EI network with microcircuit structure does not perform significantly better than the control network. Whereas the neuron model and the circuit parameters seem not to greatly influence performance, the readout method clearly has an impact. Memoryless readout causes much lower recognition rates. One might argue that the reason for this is in the appliance of the input signal to all neurons, constantly overwriting memory that otherwise would be retained in hidden neurons. To test this objection, we also examined the role of hidden neurons (Fig.2, lower panels). Extrapolating from the insight from feed-forward networks, hidden neurons are thought to enhance the computational capabilities of the network also in the case of recurrent networks. The amount of hidden neurons is tuned by randomly selecting with a probability equal to a desired input ratio a subset of neurons that will receive input, i.e. transforming those neurons into input neurons. As in [3] and [14], the connectivity was restricted to local next neighbor connections ($\lambda = 2$), except for one test using Izhikievich neurons with $\lambda = 0$. With both readout methods, we observed no benefit from hidden neurons, and, moreover, they also fail to remedy the low memoryless readout performance. If hidden neurons were beneficial to the network, we should perceive a

maximum read-out at some optimal input/reservoir neuron ratio I, which, however, is absent. In the Arabic Digit task at $\lambda = 0$ we observe for memoryless readout that the performance does not consistently increase with the number of actually used neurons (i.e., beyond $I = 0.1$, see 'Izhikevich *'). This suggests that nonlinear effects between the input components do not enhance recognition (with $I = 0.1$ there are on average 13.5 neurons that receive input while the input dimensionality is 13). In the Auslan task we see a monotonous recognition rate dependence on input neuron ratio, which can be explained by the fact that for most ratios I the number of neurons that receive input is smaller than the input dimensionality (i.e., $I \cdot 135 < 95$).

LEI networks were used in a third experiment (Figure 3) to examine the impact of the biological layering details, by comparing it to a randomized version. No significant effect on performance emerges when using the biological circuit compared to a purely random one. Hence the layer segregation and the special interlayer connectivity of this circuit does not lead to an improvement over the monolithic random circuit. The overall lower performance of both of this circuits versus the EI circuits in the case of the integration method is a result of the sparseness of input and output neurons (right parts of Figure 2 vs. Figure 3). Here LIF neurons outperform Izhikevich neurons.

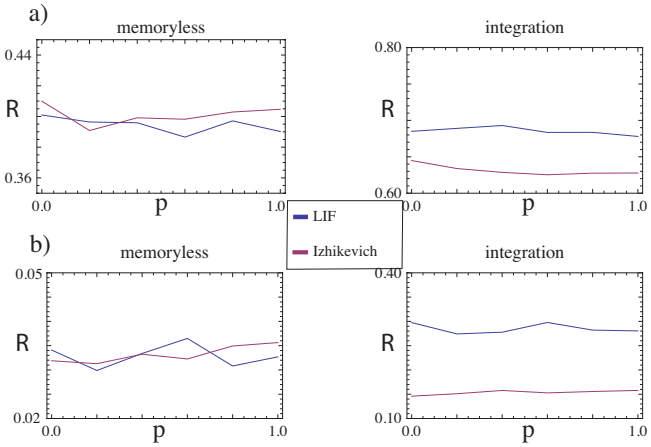

Figure 3: Recognition rate R of LEI networks with rewiring probability p ($p = 0$: layered microcircuit, $p = 1$: homogeneous control circuit). a) Arabic digit recognition, b) Auslan Sign recognition. We observe an indifference towards random rewiring of the microcircuit structure.

We found no evidence of bio-inspired connection structures influencing LSM performance. In stimuli separation tasks, LSM even with no connections or synapses performed almost equally well. We also noted that the original LSM with memoryless readout performs worse than LSM with integrated output. Recent theoretical results may offer an explanation of this phenomenon. In Ref. [15] it was found that generic recurrent networks have very low memory capacity when scaled by the number of neurons. If the input matrix W_{in} is not exactly tuned to the recurrence matrix W, the network's memory capacity is the same as that of an ensemble of entirely disconnected neurons. Only networks with linear neurons and intrinsic long feed-forward connectivity show a substantially increased memory capacity. Against this background, it is not surprising that also biologically inspired circuits cannot not per se resolve this situation.

For technical applications of LSM, we conclude that the readout method must be carefully chosen with respect to the application. In the present work, following and focusing on biological blueprints, we did not tune our LSM for optimal performance. Much higher recognition rates could have been achieved, by choosing a larger number of neurons and optimized time constants. In this sense, we emphasize that our work does not exhibit a deficiency of the ESM/LSM networks, but speaks against a too simplistic or too wide computational interpretations of the physiological facts of the columnar organization of the mammalian brain.

References

[1] Jaeger, H. (2007). *Scholarpedia*, vol. 2, 2330, 2007.

[2] Lukoševičius, M., & Jaeger, H. *Computer Science Review*, vol. 3, 127-149, 2009.

[3] Maass, W., Natschlaeger, T., & Markram, H. *Neural Computation*, vol. 14, pp. 2531-2560, 2002.

[4] Maass, W., Natschlaeger, & T., Markram, H. *Computational Neuroscience: A Comprehensive Approach*, pp. 575-605, 2003.

[5] Bertschinger, N., & Natschlaeger, T. *Neural Computation*, vol. 16, pp. 1413-1436, 2004.

[6] Haeusler, S., & Maass, W. *Cerebral Cortex*, vol. 17, pp. 149-162, 2007.

[7] Schrauwen, B., Buesing, L., & Legenstein, R. *Neural Information Processing Systems* Conference 2008.

[8] Buesing, L., Schrauwen, B. & Legenstein, R. *Neural Computation*, vol. 22, pp. 1272-1311, 2010.

[9] Izhikevich, E. *IEEE Transactions on Neural Networks*, vol. 14, pp. 1569-1572, 2003.

[10] Hammami, N., & Sellami, M. Proc. IEEE ICITST09 Conference, pp. 1-4, 2009.

[11] Kadous, M. PhD Thesis, School of Computer Science and Engineering, University of New South Wales, 2002.

[12] Frank, A. & Asuncion, A. UCI Machine Learning Repository, http://archive.ics.uci.edu/ml, University of California, School of Information and Computer Science, Irvine, 2010.

[13] Fette, G., & Eggert, J. *Proceedings of the 15th International Conference on Artificial Neural Networks*, ICANN 2005 LNCS, vol. 3696, Springer, pp. 13-18, 2005.

[14] Verstraeten, D., Schrauwen, B., Stroobandt, D., & Van Campenhout, J. *Information Processing Letters*, vol. 95, pp. 521-528, 2005.

[15] Ganguli, S., Huh, D., & Sompolinsky, H. *Proc. Natl. Acad. Sci. USA*, vol. 105, pp. 18970-18975, 2008.